

# Crystal Structure of Interleukin-19 Defines a New Subfamily of Helical Cytokines\*

Received for publication, August 22, 2002, and in revised form, October 22, 2002  
Published, JBC Papers in Press, October 25, 2002, DOI 10.1074/jbc.M208602200

Changsoo Chang‡, Eugenia Magracheva§, Serguei Kozlov¶, Steven Fong||, Gregory Tobin||, Sergei Kotenko\*\*, Alexander Wlodawer‡, and Alexander Zdanov‡ ‡‡

From the ‡Protein Structure Section, Macromolecular Crystallography Laboratory, Center for Cancer Research, NCI-Frederick, National Institutes of Health, the §Intramural Research Support Program, SAIC-Frederick, Inc., and the ¶Cancer and Developmental Biology Laboratory, NCI-Frederick, National Institutes of Health, Frederick, Maryland 21702-1201, ||Biological Mimetics, Inc., Frederick, Maryland 21702, and the \*\*Department of Biochemistry and Molecular Biology, University of Medicine and Dentistry of New Jersey, New Jersey Medical School, Newark, New Jersey 07103-2714

**Interleukin-19 (IL-19) is a novel cytokine that was initially identified during a sequence data base search aimed at finding potential IL-10 homologs. IL-19 shares a receptor complex with IL-20, indicating that the biological activities of these two cytokines overlap and that both may play an important role in regulating development and proper functioning of the skin. We determined the crystal structure of human recombinant IL-19 and refined it at 1.95-Å resolution to an R-factor of 0.157. Unlike IL-10, which forms an intercalated dimer, the molecule of IL-19 is a monomer made of seven amphipathic helices, A–G, creating a unique helical bundle. On the basis of the observed structure, we propose that IL-19, IL-20, and other putative members of the proposed IL-10 family together form a distinct subfamily of helical cytokines.**

The identification of IL-19<sup>1</sup> as a secreted protein and a cytokine (1) is based on several features such as its production by immune cells, its ability to be secreted from cells, and its capacity to induce Jak-STAT signal transduction pathway through a specific receptor complex (1, 2). It has been postulated that IL-19, IL-10, IL-20, IL-22, IL-24, IL-26, and several virus-encoded cytokines together form the IL-10 family (3–5).

IL-19 signals through a receptor complex that is also utilized by IL-20 and IL-24 (2, 6, 7). The complex is composed of two chains, CRF2–8 (or IL-20R1) and CRF2–11 (or IL-20R2; Refs. 2–8), belonging to the class II cytokine receptor family (9, 10). Receptors from this family also form heterodimeric complexes for type I and type II interferons and for other IL-10-related cytokines. Tissue factor, which binds coagulation factor VIIa, also makes use of receptors belonging to this family. Binding of IL-19 to the receptor complex results in STAT3 phosphoryla-

tion and subsequent activation of a reporter gene controlled by a minimal promoter containing STAT-binding sites (2).

The transcription of the IL-19 gene has been detected in resting monocytes and, at lower level, in B cells (11); it is up-regulated in monocytes stimulated with lipopolysaccharide or granulocyte-macrophage colony-stimulating factor (1, 11). Priming monocytes with IL-4 or IL-13 but not with interferon- $\gamma$  significantly increases the levels of IL-19 mRNA induced by subsequent lipopolysaccharide treatment (1). IL-19 mRNA also has been detected in Epstein-Barr virus-transformed lymphocytes (1, 11), suggesting that viral infection can induce IL-19 expression in certain cells. The pattern of expression of IL-19 receptor subunits can reveal the site for IL-19 action. Because the simultaneous presence in a cell of both receptor subunits CRF2–8 (IL-20R1) and CRF2–11 (IL-20R2) is required for IL-19 activity, only tissues in which the expression of both subunits has been detected can be considered a potential target for IL-19 action. IL-20R2 has a more limited pattern of expression than IL-20R1 (7), and thus the expression of IL-20R2 should be a limiting factor dictating the physiological sites of action of IL-19. Expression of mRNAs for both receptors, although at different levels, has been detected in the skin, testis, ovary, heart, lung, muscle, placenta, adrenal gland, small intestine, and salivary gland (7). The expression of the IL-19 receptor subunits in skin is of a particular interest because it has been found to be up-regulated in psoriatic skin, whereas normal skin has low levels of receptor expression. The expression of receptors also has been detected in keratinocytes, endothelial cells, and immune cells in psoriatic lesions. Moreover, IL-20-transgenic mice die within days after birth with skin abnormalities characteristic for psoriasis (7). Sharing of the same receptor complex by both IL-19 and IL-20 suggests that IL-19 should have overlapping biological activities with IL-20 and thus may be a player in psoriatic lesions. Therefore, the pattern of expression of IL-19 and its receptors suggests that this cytokine may be involved in the regulation of inflammatory responses in various tissues and may be particularly important for proper skin development and functioning.

Genes encoding IL-10-related cytokines are clustered on human chromosomes 1 and 12 and possess similar structural organization (4), indicating that they evolved from a common predecessor. Structural homology of the genes for IL-10-related cytokines also extends to the limited homology of amino acid sequences of the cytokines in the 20–40% range. At present, the structures of IL-10 and two of its virally encoded analogs have been solved, and they represent intercalating homodimers (12–16). By contrast, the recently solved structure of IL-22 (17) shows that this cytokine, although a crystallographic dimer, is

\* This work was supported in part by NCI, National Institutes of Health Contract NOI-CO-12400. The costs of publication of this article were defrayed in part by the payment of page charges. This article must therefore be hereby marked "advertisement" in accordance with 18 U.S.C. Section 1734 solely to indicate this fact.

The atomic coordinates and structure factors (code 1N1F) have been deposited in the Protein Data Bank, Research Collaboratory for Structural Bioinformatics, Rutgers University, New Brunswick, NJ (<http://www.rcsb.org/>).

‡‡ To whom correspondence should be addressed: Macromolecular Crystallography Laboratory, NCI-Frederick, P. O. Box B, Frederick, MD 21702-1201. Tel.: 301-846-5344; Fax: 301-846-7101; E-mail: zdanov@ncifcrf.gov.

<sup>1</sup> The abbreviations used are: IL, interleukin; STAT, signal transducers and activators of transcription; CRF, corticotropin-releasing factor; R1, receptor 1; R2, receptor 2.

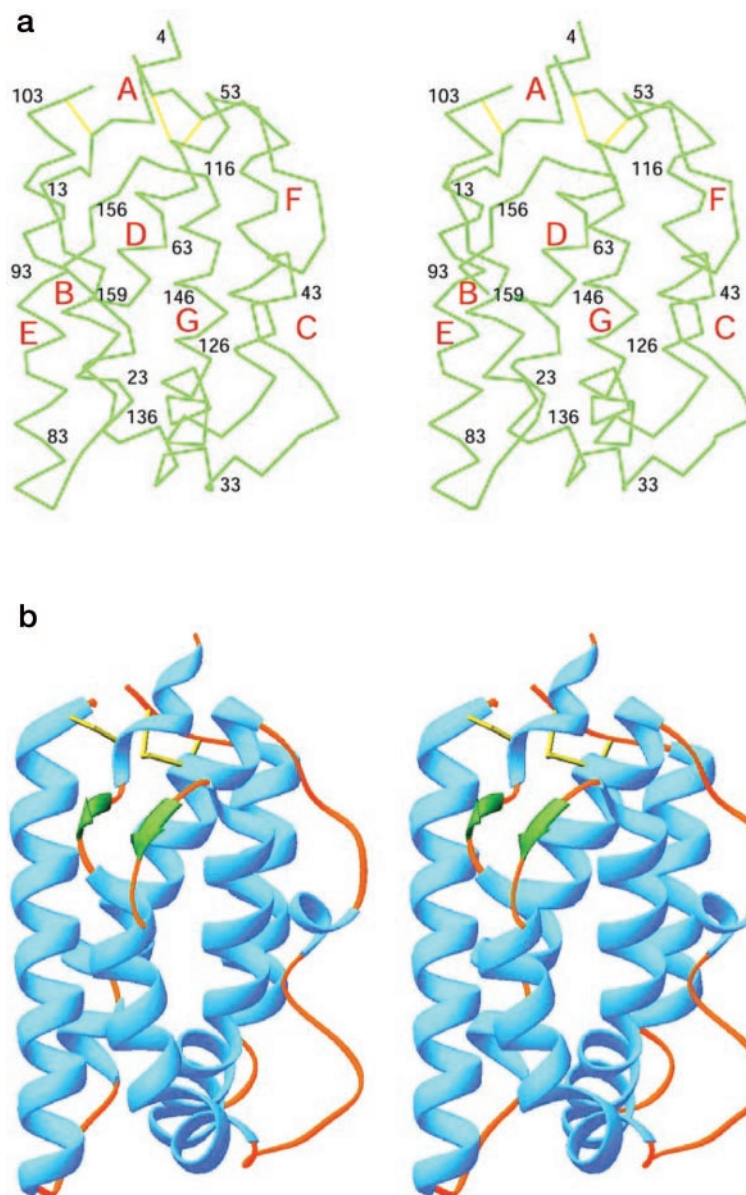


FIG. 1. Crystal structure of IL-19. *a*, stereo tracing of the C $\alpha$  atoms of IL-19. The backbone is shown in green, the disulfide bridges are shown in yellow, and the  $\alpha$  helices are labeled as A–G. *b*, stereo ribbon representation of IL-19.

a monomer both in solution and as a biological unit. Here we report the crystal structure of IL-19 (Fig. 1) at the resolution 1.95 Å. Similar to IL-22 but unlike IL-10, IL-19 was found to be a monomer both in the solution and in the crystal, and we conclude that the subgroup of cytokines of which it is a member should be considered structurally quite distinct from IL-10 itself.

#### EXPERIMENTAL PROCEDURES

**Expression and Purification of IL-19**—Schneider-2 cells were propagated in Insect Express medium (BioWhittaker, Inc., Walkersville, MD) supplemented with 5% fetal bovine serum. The human cDNA gene encoding interleukin-19 and corresponding to amino acid residues 1–159 (IL-19, GenBank™ accession number AY040367) was furnished with a sequence coding for the *Drosophila* signal peptide followed by a His<sub>6</sub> affinity purification tag. An artificial opal TGA stop codon was engineered at the 3' end of the expression fragment along with *Kpn*I and *Eco*RI restriction sites on its 5' and 3' ends, respectively. The construct was cloned into the constitutive insect cell expression vector pAc5.1/V5-HisA (Invitrogen). Schneider-2 cells ( $\sim 1 \times 10^6$  cells) were co-transfected with the resulting vector and pCo-Hygro (Invitrogen) using the cationic lipid Maxfect (Molecular Research Laboratories, Inc., Herndon, VA). Every 3 days following transfection, culture medium containing hygromycin B (300  $\mu$ g/ml) was refreshed. Drug selection continued in tissue culture plates and flasks until the hygromycin-

resistant population had expanded to  $\sim 1 \times 10^8$  cells. After selection, the cells were propagated as spinner cultures at cell densities between  $1 \times 10^6$ /ml and  $5 \times 10^7$ /ml without antibiotics. Conditioned supernatants containing recombinant IL-19 were concentrated and dialyzed against 20 mM sodium phosphate buffer, 0.5 M NaCl, pH 7.0 (buffer A). Purification was carried out by using a HiTrap Chelating 5-ml column charged with Ni<sup>2+</sup>. Protein solution was put on the column with a peristaltic pump at a flow rate of 2 ml/min. The column was washed extensively with buffer A followed by buffer A plus 10 mM imidazole; elution of the protein was accomplished with buffer A plus 50 mM imidazole. The final material was obtained by Superdex 75 gel filtration in 50 mM HEPES, 200 mM NaCl, pH 7.0. A STAT activation electrophoretic mobility shift assay showed that the protein was fully active in comparison with IL-19 produced by COS cells.

**Crystallization, Data Collection, and Structure Determination**—Crystallization conditions were initially found from Hampton Research crystallization kit I at 21 °C, tube number 4. However, final crystals were obtained by the hanging drop method in 100 mM HEPES, 1.9 M ammonium sulfate, 2% polyethylene glycol 400, pH 6.9. The protein concentration was 7 mg/ml. Crystals were grown for 2 months and were flashed in 25% (w/v) glycerol/well solution before freezing at 100 K. Diffraction data for both the native crystals and heavy atom derivatives were collected on a MAR-345 image plate system coupled with an RU-200 x-ray generator. Crystals belong to the orthorhombic system, space group P2<sub>1</sub>2<sub>1</sub>2<sub>1</sub>, with one molecule/asymmetric unit. Unit cell parameters are  $a = 30.7$  Å,  $b = 53.0$  Å, and  $c = 93.5$  Å. The programs

TABLE I  
Data collection, phasing, and refinement statistics

Data collection			
Data set	Native	EMP <sup>c</sup>	UO <sub>2</sub> Cl <sub>2</sub>
Resolution (Å)	45–1.95	45–3.5	45–3.5
Unique reflections	10,032	2198	2160
Completeness (%)	83.6	99.2	98.0
I/σ(I)	15.8	17.2	17.9
R <sub>sym</sub>	0.065	0.096	0.063
Phasing			
Number of sites		2	1
FOM <sup>a</sup>	0.55		
FOM after RESOLVE	0.70		
Refinement			
R <sub>work</sub> /R <sub>free</sub>	0.156/0.243		
r.m.s. <sup>b</sup> deviations			
Bonds (Å)	0.018		
Angles (°)	1.9		

<sup>a</sup> Figure of merit.

<sup>b</sup> Root mean square.

<sup>c</sup> Ethyl mercuric phosphite.

DENZO and SCALEPACK (18) were used for data processing. Phase determination was carried out with the programs PHASES (19) and SOLVE/RESOLVE (20) by using two isomorphous derivatives at 3.5-Å resolution (Table I). An electron density map obtained using RESOLVE allowed us to generate the initial model, which contained about 60% of the amino acid residues. The rest of the molecule was placed during alternating cycles of refinement and map fitting. The refinement at high resolution was carried out with the software program CNS (21), and the maps were fitted with the program O (22). The final model contains residues 4–104 and 108–159, 164 water molecules, and a single *N*-acetylglucosamine attached to Asn<sup>38</sup>. The coordinates have been deposited in the Protein Data Bank (accession code 1N1F).

## RESULTS AND DISCUSSION

**Description of IL-19 Molecule**—The crystal structure of IL-19 was solved by a multiple isomorphous replacement technique by using two heavy atom derivatives (Table I) at the resolution 3.5 Å and was later refined using full resolution of the available data (1.95 Å). The final structure consists of residues 4–104, residues 108–159, and 164 water molecules. All residues have conformations corresponding to either most favorable (93%) or allowed (7%) regions on the Ramachandran plot (Fig. 2). Of the two predicted glycosylation sites, Asn<sup>38</sup> and Asn<sup>117</sup>, only the former was found to be occupied, whereas the latter does not appear to bind any oligosaccharide. The conclusion is based both on the lack of electron density, which could be identified as an oligosaccharide (Fig. 3), and on the observed interactions of the side chain of Asn<sup>117</sup>. Its OD1 atom makes a hydrogen bond to NH1 of Arg<sup>120</sup>, whereas the ND2 atom is hydrogen-bonded to the carbonyl oxygen of Gln<sup>113</sup> and to a bridging water molecule in the intermolecular interface. We were able to identify only the first *N*-acetylglucosamine moiety linked to the ND2 atom of Asn<sup>38</sup>. Even though some weak electron density beyond this saccharide suggested the presence of additional sugars, it was impossible to locate them unambiguously in the electron density because they probably have multiple conformations. In fact, even the first *N*-acetylglucosamine very likely adopts several conformations, although the orientation that we found is clearly the major one, corresponding to an occupancy rate of about 70%.

A molecule of IL-19 is a monomer made up of seven amphipathic helices, A–G, of different lengths (Fig. 1*a*), forming a unique seven-helix bundle with an extensive internal hydrophobic core. Three disulfide bridges located on the top of the bundle make the polypeptide chain framework quite rigid. Most of the helices adopt 3<sub>6,13</sub> and 3<sub>10</sub> conformations; however, kinks are seen in helices B and G, and a  $\pi$ -helical turn is present in helix D. Helices B, D, E, and G make a four-helix bundle, which is a characteristic feature of all helical cytokines

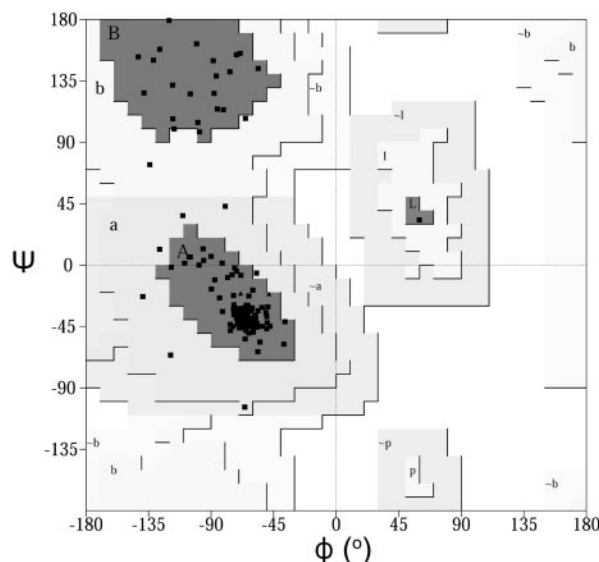


FIG. 2. Ramachandran plot for the final structure of IL-19.

(23). The position of helix A, which covers the top of the molecule, is stabilized by the disulfide bridge Cys<sup>10</sup>–Cys<sup>103</sup>, linking it covalently to the C terminus of helix E. The second and third disulfide bridges, Cys<sup>57</sup>–Cys<sup>109</sup> and Cys<sup>58</sup>–Cys<sup>111</sup>, hold together the N terminus of helix D, the interhelical loop EF, and the N terminus of helix F. The C-terminal strand 154–159 is bent along the surface of the molecule and makes hydrogen bonds with the short interhelical strand AB. These two parallel strands form a short  $\beta$ -sheet never seen previously in helical cytokines (Fig. 1*b*). Temperature factors for the protein average 37.2 Å<sup>2</sup>, whereas those for the solvent are 52.5 Å<sup>2</sup>. The highest temperature factors, indicating considerable flexibility of the molecule, are found at the N terminus and, surprisingly, in the region that contains two cysteines involved in forming separate disulfides (residues 103 and 109). Residues 105–107 were not placed in the final model, although some scattered electron density is seen in the area where they might be located. It is likely that these residues exhibit multiple conformations for both the main chain and the side chains, and thus their structure remains presently undefined.

**Comparisons with Related Cytokines**—Because IL-19 is a monomer, whereas IL-10 is an intercalated dimer consisting of two identical domains, we superimposed the coordinates of IL-19 onto one of the domains of IL-10. The root mean square deviation between the positions of C $\alpha$  atoms is only 1.7 Å, and it can easily be improved even further if we remove the N-terminal 14 residues of IL-19 (helix A), the first 21 residues of IL-10, the C-terminal 6 residues, and a few residues in the interhelical loops, particularly at the top of the molecule (Fig. 4). The orientation of helix E (helix D of IL-10) relative to the rest of the helical bundle is also different, with the root mean square deviation at its N terminus being about 1 Å and increasing to 3.8 Å at its C terminus. The general architecture of these molecules is very much alike, although the orientation of the new helix A and the short  $\beta$ -sheet in the IL-19 make the overall shape of the molecule more compact and smooth.

A BestFit (24) comparison of the amino acid sequences of IL-19 and IL-10 shows 21% identity (30 residues) and 37.5% similarity, whereas the identity and the similarity between IL-20 and IL-10 are 29.5 and 47.3%, respectively. In both cases the identity/similarity begins at position 22 of IL-10, corresponding to the beginning of helix B of IL-19 and, very likely, of IL-20 as well. A comparison of IL-19 and IL-20 gives even better sequence homology between them (44.1% identity, 52.4%

FIG. 3. The final  $2F_o - F_c$  electron density map in the area of the second putative glycosylation site, Asn<sup>117</sup>. Atoms are color-coded as follows: carbon atoms are green, nitrogen atoms are blue, and oxygen atoms are red. All residues and water molecules belonging to the symmetry-related molecules are violet. Possible interactions of the side chain atoms of Asn<sup>117</sup> (distances less than 3.5 Å) are shown as dashed lines. The contour level is 1.0  $\sigma$ . Wat, water.

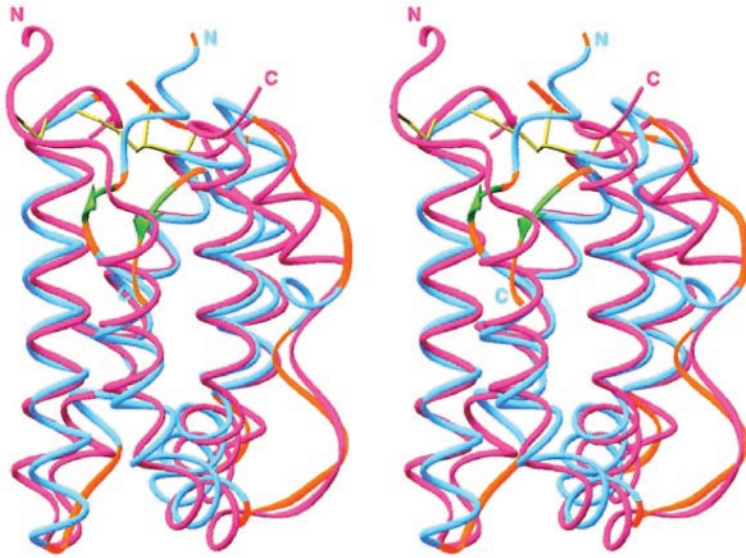
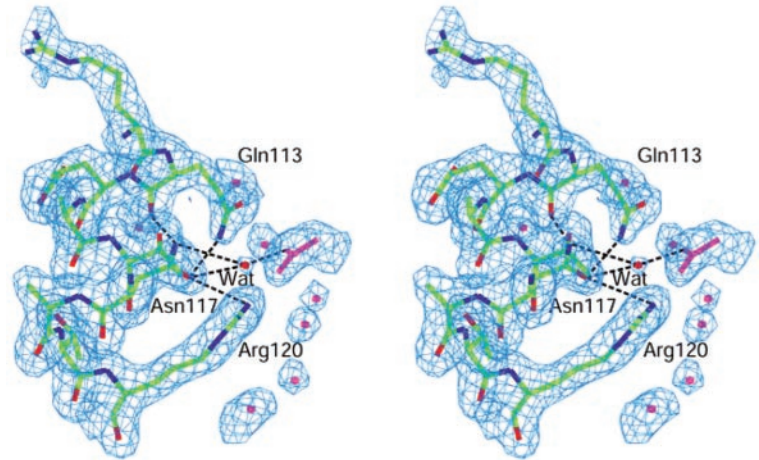


FIG. 4. Stereo diagram of the superposition of IL-19 with a single domain of IL-10. Ribbons are cyan, coils are brown, and  $\beta$ -strands are green. IL-10 is represented in pink, and disulfide bonds are shown in yellow.

similarity) without any gaps or deletions, starting earlier in the sequence (Fig. 5) at the position corresponding to helix A of IL-19. It is interesting that to achieve the best quality of alignment, one only needs to shift the amino acid sequence of IL-20 four positions to the left along the sequence of IL-19 (Fig. 5). The superposition of the sequences of all three proteins shows a remarkable degree of similarity in the positions of hydrophobic residues and of the cysteines involved in the formation of the disulfide bridges. In fact, all three disulfide bonds present in IL-19 are also preserved in IL-20. We must conclude that, taken together, the three-dimensional structure of IL-20 must be similar to IL-19, and it is no surprise that these two cytokines share their receptors. The only obvious difference between IL-19 and IL-20, besides their N termini, is expected at the C terminus in the region of the C-terminal  $\beta$ -strand of IL-19. There is no such strand in IL-20 because Glu<sup>157</sup>, the last residue of IL-20, corresponds to His<sup>153</sup> of IL-19, which is the last residue in the helix G.

The identity between IL-19 and IL-24 (MDA-7) is slightly lower at 31% with 40% similarity. Interestingly, the latter cytokine has only two cysteines (Cys<sup>16</sup> and Cys<sup>63</sup>), corresponding to Cys<sup>10</sup> and Cys<sup>57</sup> of IL-19. Since these two cysteines are involved in making separate disulfide bonds and their C $\alpha$  positions are 8.6 Å apart, this must indicate either that IL-24 forms a monomer with a very unique conformation of the N terminus, bringing Cys<sup>16</sup> into the proximity of Cys<sup>63</sup> to form a disulfide bridge between them, or that IL-24 is a

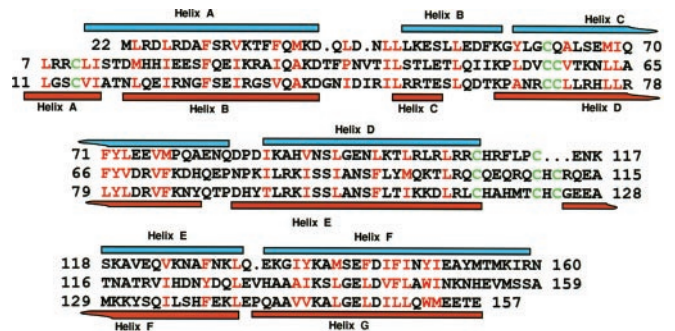


FIG. 5. Sequence alignment of IL-10 (top), IL-19 (middle), and IL-20 (bottom). Conservative hydrophobic residues are marked in red, whereas cysteines are green. Helices of IL-10 and IL-19 are shown in cyan and red, respectively.

dimer stabilized by inter-monomer disulfide bridges similar to those found in the structure of the cytomegalovirus homolog of IL-10 (16).

The sequence similarity between IL-19 and IL-22 is not as high as the sequence similarity between either IL-19 and IL-20 or IL-19 and IL-24; however, there is still 36% sequence similarity if the gap penalty (24) is allowed to be lower. A superposition of the structures of IL-19 and IL-22 (17) results in a root mean square deviation of 1.7 Å for 123 pairs of C $\alpha$  atoms. This value is almost identical to the results of the superposition of

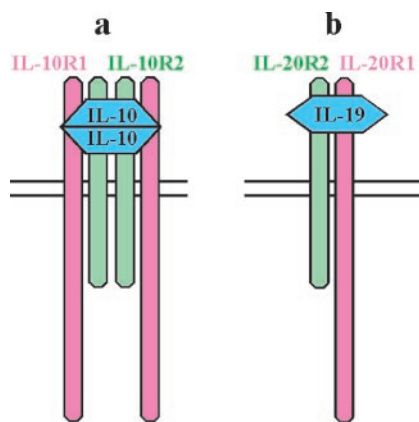


FIG. 6. Schematic diagram of the IL-10 and IL-19 receptor complexes. *a*, an IL-10 homodimer interacts with four receptor subunits, two molecules of IL-10R1, and two molecules of IL-10R2. *b*, an IL-19 monomer is likely to signal through heterodimeric receptor complexes consisting of IL-20R1 and IL-20R2 subunits.

IL-19 and IL-10, although the overall similarity appears to be higher because of the monomeric nature of both molecules. Whereas the disulfide bridge Cys<sup>10</sup>–Cys<sup>103</sup> of IL-19 corresponds to the disulfide bridge Cys<sup>7</sup>–Cys<sup>99</sup> of IL-22, they are also significantly shifted (2.5–5.5 Å for the respective C $\alpha$  coordinates). Although IL-19 Cys<sup>57</sup> is equivalent in sequence to Cys<sup>56</sup> of IL-22, their C $\alpha$  coordinates are 3.3 Å apart, and their disulfide partners are different. A similar variability of the disulfides has previously been reported for short-chain helical cytokines (25). Another structural feature very highly conserved between these cytokines is a salt bridge formed between Lys<sup>27</sup> and Asp<sup>143</sup> and located on the surface of the molecule. This bridge is strictly conserved in IL-19, IL-10, IL-22, and IL-24, with a mutation to Arg in IL-20.

**Receptor-binding Sites**—The functional IL-10 ligand-receptor complexes contain a dimer of ligands, two copies of the IL-10R1 subunit, and likely two copies of the IL-10R2 subunits (Fig. 6; Refs. 8, 26, and 27). In the case of IL-19, two subunits, IL-20R1 and IL-20R2, are required to assemble a functional receptor complex. Although it is not clear yet what sequence of events takes place on the cell surface, it is known that IL-19 makes a stable ternary complex with both receptors at the same time (2). This is similar to what has been shown for the binding of IL-20 with IL-20R1 and IL-20R2 (7). Nevertheless, because the superposition of IL-19 onto one domain of the dimer of IL-10 is so good (Fig. 4), it is appropriate to speculate that the receptor-binding site on IL-19 surface should be somewhat similar to that of IL-10. We marked the receptor-binding site of IL-19 by using crystal structure of the complex of IL-10 with its soluble non-glycosylated mutant of IL-10R1 (27). It is interesting that a simple substitution of the IL-10 domain with IL-19 in the structure of the IL-10/IL-10R1 complex gives a quite reasonable model for ligand/receptor interactions. The only clash occurs between Glu<sup>46</sup> of IL-10R1 (loop L2) and Asn<sup>38</sup>, which is the glycosylation site of IL-19 with attached oligosaccharide. There are also a few close contacts in the area of the C-terminal strand of IL-19 and loops L5 and L6 of the receptor. Table II shows all residues of IL-19 within the range of 5 Å from the receptor. Residues interacting with the receptor are located on helix B, loop BC, helix C, helix G, and the C-terminal  $\beta$ -strand, including carboxyl oxygens. It is very likely that one of the receptor interaction sites in IL-19 is similar to that in IL-10. Whether this site contacts the IL-20R1 or IL-20R2 subunit of the IL-19 receptor complex remains to be seen.

**IL-19 Defines a Distinct Subfamily of Cytokines**—IL-19

TABLE II  
Amino acid residues of IL-19 within the range of 5 Å from the receptor

Amino acid residue	Location	Amino acid residue	Location
Asp <sup>15</sup>	Helix B	Thr <sup>40</sup>	Loop BC
Met <sup>16</sup>	Helix B	Glu <sup>46</sup>	Helix C
His <sup>17</sup>	Helix B	Lys <sup>137</sup>	Helix G
Glu <sup>20</sup>	Helix B	Gly <sup>140</sup>	Helix G
Glu <sup>21</sup>	Helix B	Glu <sup>141</sup>	Helix G
Gln <sup>24</sup>	Helix B	Asp <sup>143</sup>	Helix G
Lys <sup>27</sup>	Helix B	Val <sup>144</sup>	Helix G
Arg <sup>28</sup>	Helix B	Asn <sup>150</sup>	Helix G
Gln <sup>31</sup>	Helix B	Val <sup>155</sup>	C-terminal $\beta$ -strand
Ala <sup>32</sup>	Helix B	Met <sup>156</sup>	C-terminal $\beta$ -strand
Asp <sup>34</sup>	Helix B	Ser <sup>157</sup>	C-terminal $\beta$ -strand
Pro <sup>37</sup>	Loop BC	Ser <sup>158</sup>	C-terminal $\beta$ -strand
Asn <sup>38</sup> -NAG <sup>a</sup>	Loop BC	Ala <sup>159</sup>	C-terminal $\beta$ -strand
Val <sup>39</sup>	Loop BC		

<sup>a</sup> *N*-acetylglucosamine.

shares 20–40% sequence identity with other members of the postulated family of IL-10-related cytokines; members of this family include IL-10, IL-20, IL-22, IL-24, and IL-26 (3, 4, 28). The expression of the IL-19 gene appears to have complex regulation. It is likely that there are two alternative promoters that may be differentially regulated. IL-19 transcripts produced from these promoters differ in their 5' untranslated regions. Translation of the IL-19 mRNA with the shorter 5' untranslated region generates IL-19 protein with a classical signal peptide, which is predicted to be 18 amino acids long and to yield Ser as a first amino acid of the secreted mature IL-19 protein. However, an alternative 24-residue-long signal peptide has been annotated in the Swiss Protein Database under Swiss-Prot accession number Q9UHD0. Until now, the identity of the first amino acid of the mature protein has not been determined experimentally, although the N terminus at position 19 is more likely based on the similarity with IL-10. The longer 5' sequence contains an additional ATG codon in-frame with the main peptide sequence. Initiation of translation from this potential alternative ATG codon produces protein with a long abnormal signal peptide affecting its secretion. We expressed IL-19 corresponding to a normal length signal peptide, with Ser as the first residue and the whole protein 159 residues long. There are two potential sites for *N*-linked glycosylation, Asn<sup>38</sup>–Val<sup>39</sup>–Thr<sup>40</sup> and Asn<sup>117</sup>–Ala<sup>118</sup>–Thr<sup>119</sup>, although we found that only the Asn<sup>38</sup> site is occupied by an oligosaccharide.

IL-19, together with IL-10 and the other cytokines mentioned above, are members of the class of long helical cytokines (25) that utilize class II receptors. Another member of that class is interferon- $\gamma$ . Whereas IL-10 and interferon- $\gamma$  form intercalating noncovalent homodimers (12–14, 29), IL-19 is monomeric. The structure presented here shows that IL-19 is a compact, seven-helix bundle with an extensive hydrophobic core inside. It is very likely that IL-20 has a very similar structure, as does IL-22. The other two newly discovered homologs of IL-10 (IL-24 and IL-26) are probably homodimers, as reported directly for IL-26 (30). Our analysis of the amino acid sequence of IL-24 suggests that this cytokine could be a covalently bound dimer. IL-24 has only two cysteines, Cys<sup>16</sup> and Cys<sup>63</sup>. Provided that its three-dimensional structure is similar to that of IL-10, it is very likely that Cys<sup>63</sup>, located at the N terminus of helix C (IL-10 notation), makes a disulfide bridge with Cys<sup>63</sup> of the second monomer in a manner similar to what has been seen in the structure of the cytomegalovirus homolog of IL-10 (16). In this case Cys<sup>16</sup> would be left free, a very unusual arrangement for helical cytokines. For that reason, we postulate that there is still a possibility that Cys<sup>16</sup> could somehow be positioned in the proximity of Cys<sup>63</sup> and form a disulfide

bridge with it. In this case IL-24 would be a monomer similar to IL-19. We may conclude that, taken together, IL-19, IL-20, IL-22, and probably also IL-24 could be united in a single subfamily of helical cytokines.

## REFERENCES

- Gallagher, G., Dickensheets, H., Eskdale, J., Izotova, L. S., Mirochnitchenko, O. V., Peat, J. D., Vazquez, N., Pestka, S., Donnelly, R. P., and Kotenko, S. V. (2000) *Genes Immun.* **1**, 442–450
- Dumoutier, L., Leemans, C., Lejeune, D., Kotenko, S. V., and Renauld, J.-C. (2001) *J. Immunol.* **167**, 3545–3549
- Dumoutier, L., and Renauld, J.-C. (2002) *Eur. Cytokine Netw.* **13**, 5–15
- Kotenko, S. V. (2002) *Cytokine Growth Factor Rev.* **13**, 223–240
- Fickenscher, H., Hor, S., Kupers, H., Knappe, A., Wittmann, S., and Sticht, H. (2002) *Trends Immunol.* **23**, 89–96
- Wang, M., Tan, Z., Zhang, R., Kotenko, S. V., and Liang, P. (2002) *J. Biol. Chem.* **277**, 7341–7347
- Blumberg, H., Conklin, D., Xu, W. F., Grossmann, A., Brender, T., Carollo, S., Eagan, M., Foster, D., Haldeman, B. A., Hammond, A., Haugen, H., Jelinek, L., Kelly, J. D., Madden, K., Maurer, M. F., Parrish-Novak, J., Prunkard, D., Sexson, S., Sprecher, C., Waggle, K., West, J., Whitmore, T. E., Yao, L., Kuechle, M. K., Dale, B. A., and Chandrasekhar, Y. A. (2001) *Cell* **104**, 9–19
- Kotenko, S. V., and Pestka, S. (2000) *Oncogene* **19**, 2557–2565
- Bazan, J. F. (1990) *Proc. Natl. Acad. Sci. U. S. A.* **87**, 6934–6938
- Thoreau, E., Petridou, B., Kelly, P. A., Djiane, J., and Mornon, J. P. (1991) *FEBS Lett.* **282**, 26–31
- Wolk, K., Kunz, S., Asadullah, K., and Sabat, R. (2002) *J. Immunol.* **168**, 5397–5402
- Zdanov, A., Schalk-Hihi, C., Gustchina, A., Tsang, M., Weatherbee, J., and Wlodawer, A. (1995) *Structure* **3**, 591–601
- Zdanov, A., Schalk-Hihi, C., and Wlodawer, A. (1996) *Protein Sci.* **5**, 1955–1962
- Walter, M. R., and Nagabhushan, T. L. (1995) *Biochemistry* **34**, 12118–12125
- Zdanov, A., Schalk-Hihi, C., Menon, S., Moore, K. W., and Wlodawer, A. (1997) *J. Mol. Biol.* **268**, 460–467
- Jones, B. C., Logsdon, N. J., Josephson, K., Cook, J., Barry, P. A., and Walter, M. R. (2002) *Proc. Natl. Acad. Sci. U. S. A.* **99**, 9404–9409
- Nagem, R. A. P., Colau, D., Dumoutier, L., Renauld, J.-C., J. C. Ogata, C., and Polikarpov, I. (2002) *Structure* **10**, 1051–1062
- Otwinowski, Z. (1993) in *Data Collection and Processing* (Sawyer, L., Isaacs, N., and Bailey, S., eds) pp. 80–86, SERC Daresbury Laboratory, Warrington, UK
- Furey, W., and Swaminathan, S. (1995) *Methods Enzymol.* **277**, 590–619
- Terwilliger, T. C., and Berendzen, J. (1999) *Acta Crystallogr. Sect. D Biol. Crystallogr.* **55**, 849–861
- Brünger, A. T., Adams, P. D., Clore, G. M., DeLano, W. L., Gros, P., Grosse-Kunstleve, R. W., Jiang, J. S., Kuszewski, J., Nilges, M., Pannu, N. S., Read, R. J., Rice, L. M., Simonson, T., and Warren, G. L. (1998) *Acta Crystallogr. Sect. D Biol. Crystallogr.* **54**, 905–921
- Jones, T. A., Zou, J. Y., Cowan, S., and Kjeldgaard, M. (1991) *Acta Crystallogr. Sect. A* **47**, 110–119
- Presnell, S. R., and Cohen, F. E. (1989) *Proc. Natl. Acad. Sci. U. S. A.* **86**, 6592–6596
- Genetics Computer Group (1994) *Program Manual for the GCG Package*, Version 8, Genetics Computer Group, Inc., Madison, WI
- Rozwarski, D. A., Gronenborn, A. M., Clore, G. M., Bazan, J. F., Bohm, A., Wlodawer, A., Hatada, M., and Karplus, P. A. (1994) *Structure* **2**, 159–173
- Kotenko, S. V., Krause, C. D., Izotova, L. S., Pollack, B. P., Wu, W., and Pestka, S. (1997) *EMBO J.* **16**, 5894–5903
- Josephson, K., Logsdon, N. J., and Walter, M. R. (2001) *Immunity* **15**, 35–46
- Josephson, K., Jones, B. C., Walter, L. J., DiGiacomo, R., Indelicato, S. R., and Walter, M. R. (2002) *Structure* **10**, 981–987
- Ealick, S. E., Cook, W. J., Vijay-Kumar, S., Carson, M., Nagabhushan, T. L., Trotta, P. P., and Bugg, C. E. (1991) *Science* **252**, 698–702
- Knappe, A., Hor, S., Wittmann, S., and Fickenscher, H. (2000) *J. Virol.* **74**, 3881–3887